



Research article

Extracellular synthesis of silver nanoparticles using cell-free culture extracts of *Aspergillus niger* QNUGT6 and evaluation of their antimicrobial activity

Nhat Hieu HOANG and Thi Mong Diep NGUYEN*

Faculty of Natural Sciences, Quy Nhon University, 170 An Duong Vuong street, Quy Nhon Nam ward, Gia Lai province, Vietnam

* **Correspondence:** Email: nguyenthimongdiep@qnu.edu.vn; Tel: +84964745083.

Abstract: Modern nanotechnology focuses on developing environmentally friendly methods for synthesizing nanomaterials. Among these, the biosynthesis of nanoparticles using biological microorganisms has emerged as a promising strategy. In this study, silver nanoparticles (AgNPs) were synthesized using the extracellular secretions of the fungus *Aspergillus niger*. The fungal strain was successfully isolated from rice wine yeast and identified as *Aspergillus niger* QNUGT6 based on morphological characterization and sequencing of the internal transcribed spacer (ITS) gene region. The formation of AgNPs was confirmed by a visible color change and the appearance of a characteristic surface plasmon resonance (SPR) band at 410 nm. X-ray diffraction (XRD) analysis revealed diffraction peaks corresponding to crystalline AgNPs. Fourier-transform infrared (FTIR) spectroscopy indicated the involvement of various functional groups in the culture medium responsible for the reduction of Ag⁺ ions to Ag⁰. Scanning electron microscopy (SEM) analysis confirmed that the synthesized AgNPs were spherical with an average size of 26.1 ± 7.8 nm. Moreover, the synthesized AgNPs exhibited inhibitory activity against *Bacillus cereus* bacterial pathogens. Thus, our study provides further evidence for the potential use of *Aspergillus* fungi to control the properties of AgNPs.

Keywords: antibacterial activity; *Aspergillus niger*; green synthesis; nanomaterial; silver nanoparticle

1. Introduction

Silver nanoparticles (AgNPs) have been used in the pharmaceutical industry since the late 19th century. Nowadays, AgNPs have been shown to be an effective treatment against a wide range of diseases, comparable to broad-spectrum antibiotics. The emergence of multidrug-resistant bacteria, along with the limited development of new antibiotics, has led to increasing awareness of the importance of AgNPs as antimicrobial agents [1].

AgNPs are particles with sizes ranging from 1 to 100 nm with unique properties, including electrical, optical, and magnetic characteristics, and notable biological activity [2,3]. Nanoparticles are capable of altering their physical, chemical, and biological properties as a function of their surface area-to-volume ratio [4,5]. This ratio significantly influences cellular uptake, biodistribution, penetration of biological barriers, and therapeutic efficacy [6–8]. Therefore, the development of AgNPs with uniformly controlled structures in terms of size, morphology, and functionality is essential for a wide range of practical applications.

The production and stabilization of nanoparticles can be achieved through physical, chemical, and biological methods. Physical methods for nanoparticle synthesis include techniques such as milling and melting, grinding, and thermal evaporation [3]. However, the drawback of physical methods is that they are very expensive due to the large amount of energy required and the low yield of nanomaterial they provide. In contrast, chemical synthesis of nanoparticles, such as electrochemical, chemical reduction, and photochemical reduction, requires low energy during reduction while producing uniform particles of controllable size and shape. However, these methods also raise significant environmental and health concerns because they involve hazardous chemicals that can cause carcinogenic, mutagenic, and cytotoxic effects [9]. These toxic substances originate from organic solvents, reducing agents, and stabilizers used to prevent unwanted aggregation of colloids. Therefore, chemical methods are unsuitable for the production of bio-nanoparticles for clinical and biomedical applications [10,11].

For these reasons, interest in bio-nanoparticle synthesis is increasing today. Notably, microbial synthesis takes place under simpler conditions and is less costly than chemical or physical methods. The resulting nanoparticles are often easy to produce, have lower toxicity, and have the desired size and shape, which is important for many applications [11–15]. Therefore, biosynthesis using microorganisms is considered a promising alternative to conventional chemical and physical methods [16]. However, to achieve good stability and biocompatibility of the obtained nanoparticles, it is important to consider the specific characteristics of the microbial strain used and optimize the synthesis conditions accordingly, such as stirring conditions, pH, culture medium, temperature, light, and incubation time. Studies have found that changes in temperature, concentration of metal precursors, pH, culture medium, and biomass amount can be used to obtain nanoparticles with different physicochemical properties [1]. Therefore, in this study, we synthesized AgNPs using an *Aspergillus niger* strain isolated from Vietnamese rice wine yeast and cultivated using the Eppendorf BioFlo 120 Bioprocess Control System. The fungal biomass was subsequently harvested and used for the synthesis of AgNPs.

On the other hand, *Bacillus cereus* is a Gram-positive, motile bacterium capable of forming endospores, which enable it to survive under harsh environmental conditions, including variations in temperature and pH, and to produce toxins that cause food poisoning. It has the ability to adhere to metal surfaces through biofilm formation and spore production, which increases its resistance to environmental factors such as pH and temperature [17]. Consequently, it can resist many common

cleaning procedures and survive cooking and reheating processes. As a result, eliminating this bacterium remains challenging in healthcare facilities, food production environments, and during food processing [18]. According to various studies, *B. cereus* has been detected in many types of food, including raw and mashed vegetables, bread, starchy foods such as rice, processed foods, milk and dairy products, and meat products [17]. However, *B. cereus* is most frequently associated with rice and rice-based foods [19], which constitute a significant part of the diet in many countries, including Vietnam, where it has been responsible for several serious cases of food poisoning. These foodborne infections are often treated with extensive use of antibiotics, but this process comes with the inherent risk of increasing bacterial antibiotic resistance. In this context, green biosynthesized AgNPs represent, among other potential biomedical applications, a promising antimicrobial alternative.

2. Materials and methods

2.1. Materials

All reagents and chemicals were purchased from Merck (China). Luria-Bertani agar media is a product of HiMedia, India. *B. cereus* was obtained from the Laboratory of Microbiology at Quy Nhon University, Vietnam. Double-distilled water was used in the experiments.

2.2. Methods

2.2.1. Isolation and identification of fungi from rice wine yeast

Rice wine yeast was finely ground, and 10 g of sample was suspended in 90 mL of sterile distilled water. The suspension was serially diluted to concentrations of 10^{-4} , 10^{-5} , and 10^{-6} . Aliquots of 0.1 mL from the 10^{-4} and 10^{-6} dilutions were spread onto Petri dishes containing potato glucose agar (PGA) medium (composition, g/L: potato extract 4 g, glucose 20 g, agar 15 g; pH 5.6 ± 0.2). These plates were incubated at 32 °C for 3 days. Then, single fungal colonies were selected and transferred to PGA medium to create pure strains. The pure fungal colonies were then sent for internal transcribed spacer (ITS) sequencing at DNA Sequencing Co., Ltd., U34C, Street No. 6, Hung Phu New Urban Area, Hung Thanh Ward, Cai Rang District, Can Tho City.

2.2.2. Bioreactor cultivation and AgNP biosynthesis

The fungal strain was cultured in PGA medium to generate biomass for the biosynthesis of AgNPs. The cultures were cultivated using the Eppendorf BioFlo 120 Bioprocess Control System. The temperature was kept constant at 32 °C. The pH 5.6 was kept constant throughout the whole cultivation by automated addition of acid (1 M HCl) and base (1 M NaOH). Batch processes were carried out for 72 h on a rotary shaker at 200 rpm and aeration to 0.2 vvm, which was sufficient to keep the dissolved oxygen (DO) concentration above 30% air saturation during all cultivations conducted. After incubation, the cultures were centrifuged at 11,000 rpm for 10 min, and the resulting supernatant was collected and used for AgNPs biosynthesis.

Silver nitrate (AgNO_3) was dissolved in sterile distilled water to prepare a 100 mM stock solution. 10 mL of 100 mM AgNO_3 solution was added to 100 mL of the cell-free filtrate in 250 mL Erlenmeyer

flasks to obtain a final AgNO₃ concentration of 10 mM. The flasks were then kept in a shaker at 150 rpm at 70 °C for 24, 48, and 96 h [8]. The formation of AgNPs was visually confirmed by a color change of the reaction mixture to brown. Control samples (cell-free filtrate without AgNO₃) were prepared simultaneously under identical experimental conditions. All reaction mixtures were stored in the dark to prevent any photochemical effects during the experiment.

2.2.3. Methods for characterizing AgNPs

The biosynthesis of AgNPs was observed using ultraviolet-visible spectrophotometry (UV-Vis) (UV-1800, Shimadzu, Tokyo, Japan) in the wavelength range of 300–800 nm.

Fourier transform infrared spectroscopy (FTIR) was used in the 4000–400 cm⁻¹ range (IRAffinity-1S Shimadzu, Japan) to detect functional groups and their possible interactions in the AgNPs biosynthesis process.

The formation of AgNPs was examined by X-ray diffraction (XRD) using an X-ray diffractometer (Bruker D2 equipped with a Cu K α radiation source).

The morphology and size of the synthesized AgNPs were determined by scanning electron microscopy (SEM) using a Hitachi S4800 SEM operated at an accelerating voltage of 5 kV.

2.2.4. Determination of AgNPs antimicrobial activity

The antimicrobial activity of the synthesized AgNPs was evaluated using the agar well diffusion method against the pathogenic microorganism *B. cereus*. Pure cultures of the test organisms were grown on sterilized Luria–Bertani agar and nutrient agar media. Ampicillin (10 μ g) and streptomycin (10 μ g) were used as controls.

Wells with a diameter of 6 mm were aseptically punched into the agar plates, and 50 μ L of the AgNPs supernatant at 96 h of incubation was added to each well by micropipette. The plates were then incubated at 37 °C for 24 h. Antimicrobial activity was assessed by the appearance of inhibition zones around the wells.

2.2.5. Determination of the minimum inhibitory concentration (MIC) and minimum bactericidal concentration (MBC)

MIC is defined as the lowest concentration of AgNPs that visibly inhibits bacterial growth, as previously described [20]. A range of AgNP concentrations (10–0.625 mM) was prepared in 96-well plates by serial dilution with nutrient culture broth. Equal volumes of the AgNP solutions and bacterial suspensions (100 μ L each) were added to each well of the plate. The bacterial suspension was adjusted to 1.5×10^8 CFU/mL (0.5 McFarland standard). The plates were then incubated at 37 °C for 24 h. The MIC value was the lowest concentration of AgNPs at which no bacterial growth was visible in the wells. The visible turbidity of the wells was recorded both before and after incubation to confirm the MIC value. All tests included wells containing only bacterial suspensions, as a growth control, and others containing only each culture broth (negative control) to ensure its sterility.

After determining the MIC, 10 μ L of samples from wells that showed no visible bacterial growth were spread onto nutrient agar (NA) plates and incubated at 37 °C for 24 h. The MBC value was the lowest concentration of AgNPs that significantly inhibited bacterial growth on the agar plates.

2.2.6. Statistical analysis

All tests were repeated at least three times. The data are presented as the mean \pm standard deviation. Data were statistically evaluated by applying an analysis of variance (one-way ANOVA) followed by a Tukey's test using the GraphPad Prism version 5.

3. Results and discussion

Among green synthesis methods for nanomaterials, fungi are considered promising agents for the synthesis of metal nanoparticles due to their ability to secrete large amounts of extracellular enzymes and proteins, which enhance the efficiency of nanoparticle formation [21]. In addition, fungi are easy to culture, require simple nutrient sources, exhibit a high metal-binding capacity on their cell walls, and can absorb metals into their cells [22–24]. Currently, the genus *Aspergillus* is widely used in nanoparticle research and production, particularly *Aspergillus niger* [8,25–36]. However, many fungal strains used in previous studies have been mainly isolated from soil, wastewater, or spoiled food and have not been thoroughly screened [25–40], which may lead to unstable enzyme activity, genetic variability, and the potential presence of genes related to toxin biosynthesis due to competitive survival pressures in natural environments. This raises concerns about the potential toxicity of the culture medium when used for the synthesis of AgNPs.

Therefore, in this study, aiming to develop an AgNPs synthesis process that is safe for human health and environmentally friendly, we isolated *Aspergillus niger* from rice wine yeast used in the traditional Vietnamese rice wine fermentation process. Fungal strains from this source have undergone natural selection in the fermentation environment and generally exhibit high enzyme production capacity (especially amylase and protease), rapid growth, good adaptation to temperature conditions, and are considered safe for food-related applications [41–43].

3.1. Isolated fungus features

The isolate was identified as a septate filamentous fungus after morphological observation, as shown in Figure 1. Colonies on potato dextrose agar (PDA) usually appear as velvety colonies with dark brown to black color due to rapid spore production, with a white or yellowish margin.

The ITS region sequencing analysis and comparison with gene banks on NCBI confirmed that the isolated strain belonged to the species *Aspergillus niger*, with a gene similarity of 100% (Table 1). The phylogenetic tree was built with MEGA 11 (Figure 2). The gene sequence was submitted to GenBank under accession no. PX788707.

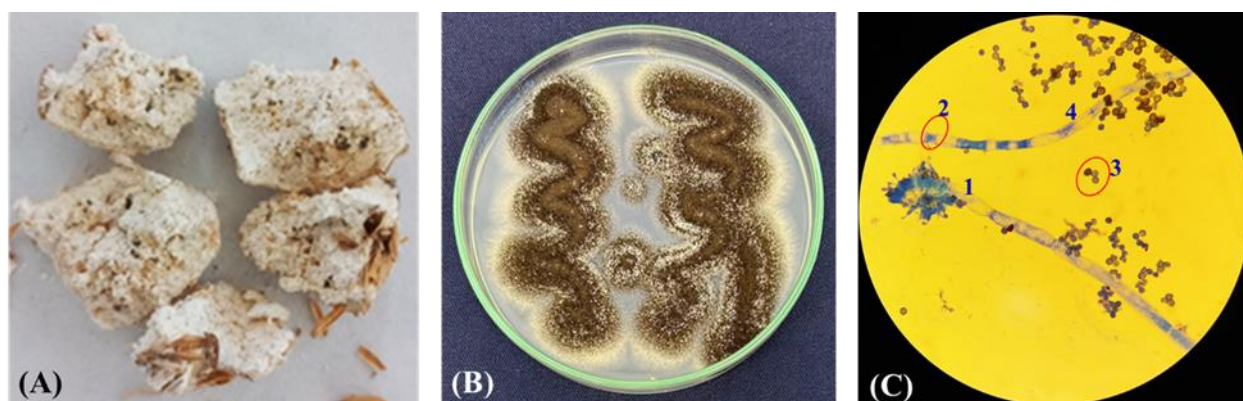


Figure 1. (A) Rice wine yeast. (B) Colonies of *Aspergillus niger* QNUGT6 strain after 5 days of culture on PGA medium. (C) Microscopic view of *Aspergillus niger* QNUGT6 isolate (100 ×) showing the conidiophore stalk (1), septum (2), conidia (3), and mycelium (4).

Table 1. Highest similarity of the ITS sequence of *Aspergillus niger* QNUGT6 compared with the reference sequence database on GenBank.

GenBank number	Species	Similarity rate	Location
MH752206.1	<i>Aspergillus niger</i> Z1A	100%	Iran
OP237078.1	<i>Aspergillus niger</i> 47N	100%	China
OP103942.1	<i>Aspergillus niger</i> C183N	100%	China
OP237082.1	<i>Aspergillus niger</i> 445N	100%	China
OQ392594.1	<i>Aspergillus niger</i> BNP14	100%	India

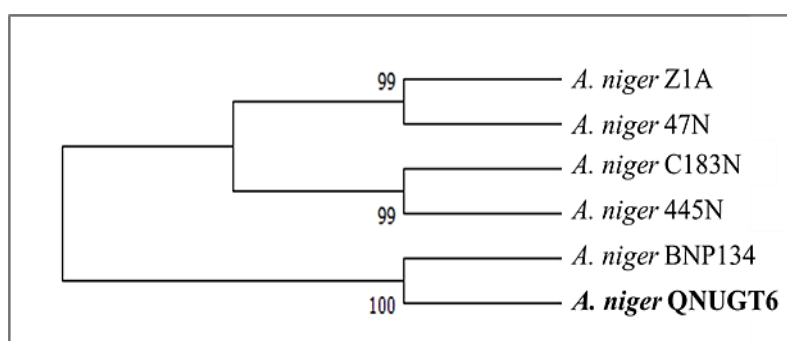


Figure 2. Phylogenetic tree showing the relationship between the studied strain and the closely related species based on ITS gene region sequences. The tree was constructed using the maximum likelihood method. Bootstrap values derived from 1000 replicates are indicated at the branch nodes, with only values above 50% shown. The results demonstrate that the studied strain clusters with representative members of the *Aspergillus niger* species.

3.2. AgNPs synthesis

The cell-free filtrate of *Aspergillus niger* QNUGT6 was mixed with AgNO₃ solution as described in the *Materials and methods* section. The light-yellow cell-free filtrate of *Aspergillus niger* QNUGT6 turned to dark brown after 24, 48, and 96 h of incubation (Figure 3), which is a primary visual indicator of AgNP biosynthesis [44–47]. In contrast, the control sample consisting of the cell-free filtrate without AgNO₃ showed no color change.

The formation of AgNPs was further confirmed by UV–Vis analysis in the wavelength range of 300–800 nm. The SPR spectrum of AgNPs exhibited a sharp and intense absorption peak at 410 nm for 24, 48, and 96 h of incubation of cell filtrate with AgNO₃, with the intensity gradually increasing with reaction time without peak shift (Figure 4). This peak confirms the presence of AgNPs, resulting from the reduction of Ag⁺ to Ag⁰ mediated by secondary metabolites produced by the fungal cells [47].

The width and frequency of SPR are influenced by several factors, including the shape and size of metal nanoparticles, the surrounding environment, and the dielectric constant of the metal [48]. For spherical nanoparticles, the SPR peak is typically observed in the wavelength range of 410–420 nm [46,48]. Moreover, an SPR peak within 400–460 nm is widely regarded as an indicator of successful AgNP synthesis [48–50]. In agreement with previous reports, AgNPs synthesized using microorganisms such as *Aspergillus sydowii*, *Lactobacillus bulgaricus*, *Arthrospira platensis*, and *Aspergillus flavus* exhibit SPR peaks between 410 and 420 nm [48,51–53].

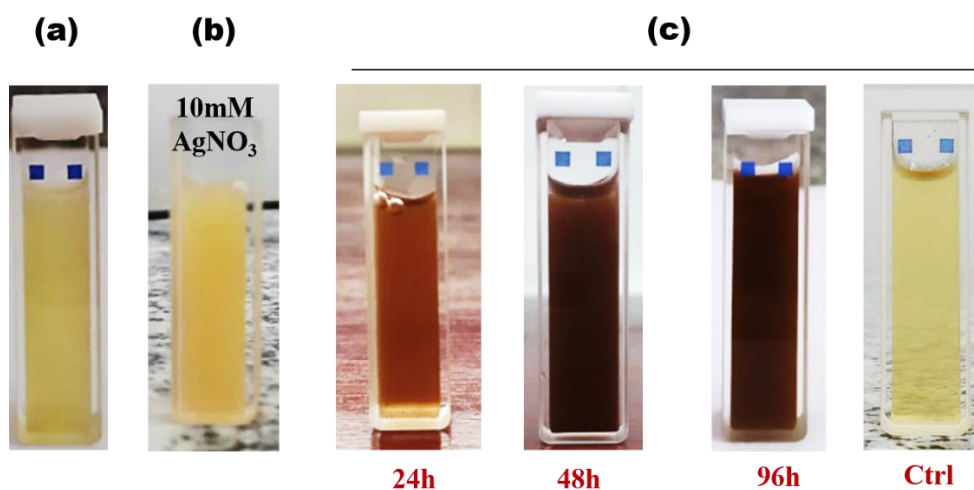


Figure 3. Erlenmeyer flasks containing cell-free filtrate of *Aspergillus niger* QNUGT6 (a) without and (b) with silver nitrate (10 mM final), and (c) with silver nitrate (10 mM final) after 24, 48, and 96 h of reaction. Ctrl: Cell-free filtrate of *Aspergillus niger* QNUGT6 without silver nitrate.

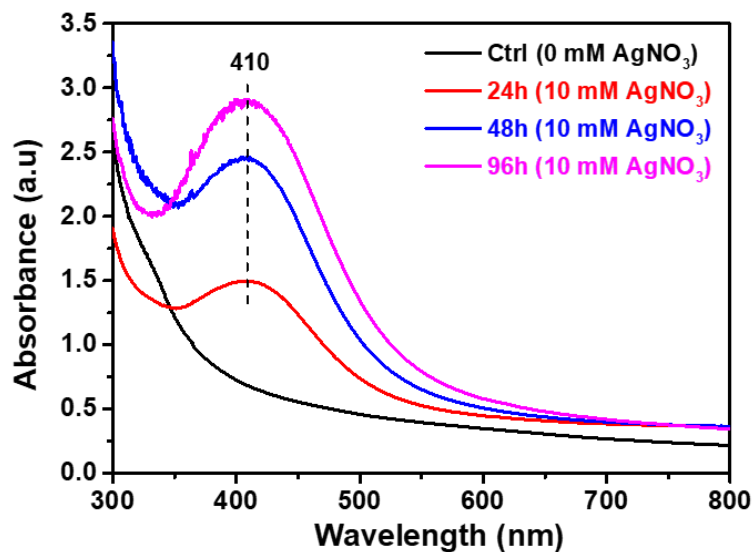


Figure 4. UV–Vis spectrum of AgNPs produced from a cell-free culture of *Aspergillus niger* QNUGT6.

3.3. Fourier transform infrared spectroscopic analysis

FTIR analysis was conducted to identify the functional groups present in the *Aspergillus niger* QNUGT6 supernatant that are involved in the reduction and stabilization of AgNPs. The FTIR spectra of the *Aspergillus niger* QNUGT6 supernatant and the synthesized AgNPs are presented in Figure 5. Infrared scanning in the range of 400–4000 cm^{-1} revealed three major absorption peaks at 1645, 3203, and 3357 cm^{-1} , which were observed in all samples, including the control without AgNO_3 .

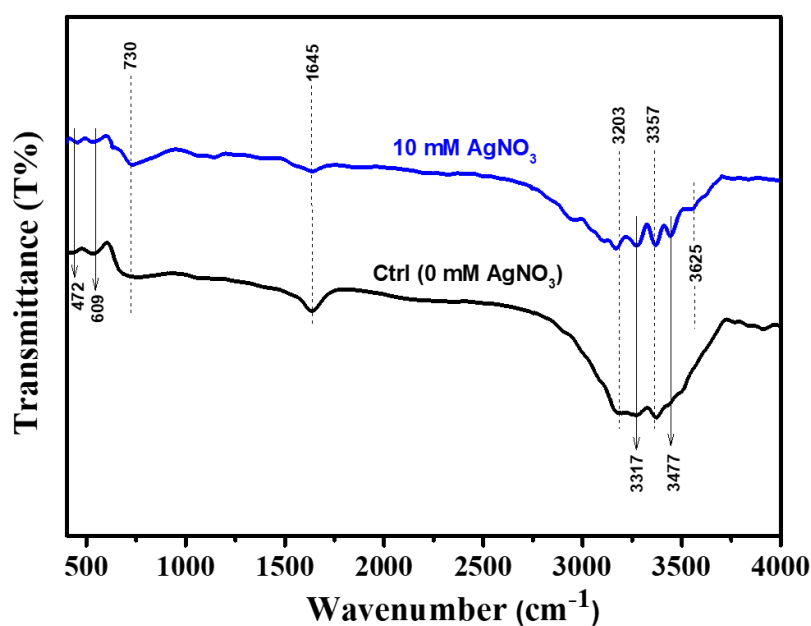


Figure 5. FTIR spectral analysis of AgNPs synthesized from the cell-free culture of *Aspergillus niger* QNUGT6.

The absorption peak at 3203 cm^{-1} is attributed to the stretching vibration of the N–H bond of amide groups in proteins, while the peak at 3357 cm^{-1} corresponds to the stretching vibration of O–H groups associated with glucose and phenolic compounds [52,54]. The absorption peak at 730 cm^{-1} acts as additional evidence for amide bond formation by representing the out-of-plane bending vibration of the N–H group [52,54]. The prominent peak at 1645 cm^{-1} corresponds to the C=O stretching vibration in the amide I region, which is characteristic of the α -helix secondary structure of proteins [55].

Previous studies have reported that amino acid residues and carbonyl peptide groups exhibit a strong affinity for metal ions and can act as capping agents, thereby preventing nanoparticle aggregation [56]. Extracellular proteins present in fungal extracts are capable of strongly binding AgNPs through free amine or cysteine groups and may play a key role in reducing Ag^+ ions to nanoscale silver particles [57].

In addition, like the control sample, the sample containing 10 mM AgNO_3 exhibited characteristic vibrational peaks at 472 cm^{-1} , which indicates S-S bond vibrations, often appearing in organic polysulfides [58], and the peak at 609 cm^{-1} indicating aromatic ring deformations [59]. Peaks observed at 3317 cm^{-1} and 3477 cm^{-1} are associated with N–H and O–H stretching vibrations of proteins, which are believed to function as stabilizing agents for AgNPs [60], and an absorption band at 3625 cm^{-1} , corresponding to O–H stretching vibrations of adsorbed water molecules [54].

Overall, the FTIR spectra of the synthesized AgNPs exhibited peaks similar to those of the fungal supernatant, albeit with reduced intensity. These results confirm the presence of bioactive molecules adsorbed on the surface of AgNPs and demonstrate the involvement of functional groups from the fungal culture medium in both the synthesis and stabilization of AgNPs.

3.4. X-ray diffraction analysis

The crystalline properties and purity of the biosynthesized AgNPs were examined using XRD. The XRD pattern of AgNPs synthesized using *Aspergillus niger* QNUGT6 is shown in Figure 6. Four distinct diffraction peaks were observed at 2θ values of 38.1° , 43.7° , 27.6° , and 32.0° , which correspond to the (111), (200), (210), and (122) crystal planes of Ag particles with a face-centered cubic structure, respectively, in accordance with the standard silver diffraction data (PDF card No. 00-004-0783) and with previously reported research results on the green synthesis of AgNPs [61–63]. The absence of impurity peaks confirms the high purity of the synthesized AgNPs.

In our previous study, AgNPs synthesized from the supernatant of another *Aspergillus niger* strain exhibited diffraction peaks at 2θ values of approximately 38.11° , 44.27° , 64.42° , and 77.47° , which correspond to the (111), (200), (220), and (311) planes, respectively [8]. These results indicate that, in microbiological synthesis, the crystalline characteristics and purity of AgNPs depend strongly on the microbial strain and the growth medium. Even within the same *Aspergillus* species, differences in strain and culture conditions can lead to variations in diffraction patterns. This variation may be attributed to the crystallization of biomolecules present in the fungal culture filtrate, which are involved in the reduction and stabilization of nanoparticles on their surface [64].

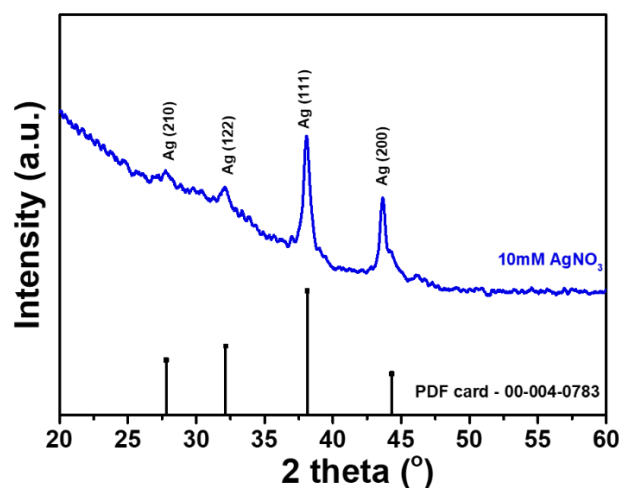


Figure 6. XRD spectrum of synthesized AgNPs from the cell-free culture of *Aspergillus niger* QNUGT6.

3.5. Scanning electron microscopy analysis

The surface morphology of the biosynthesized AgNPs was further investigated using SEM. Figure 7(a–d) presents the SEM images of the synthesized AgNPs with different incubation times of 24, 48, and 96 h, corresponding to samples (a), (b), and (c), respectively. The observations indicate that all synthesized samples consist of nearly spherical AgNPs. As the incubation time increases, the nanoparticle density increases significantly, accompanied by partial agglomeration; however, the particle size shows no substantial variation. The average particle size, estimated by plotting a histogram (Figure 7e) with the aid of ImageJ software, was found to be 26.1 ± 7.8 nm from image (d), which is a magnified SEM image of sample (a). The nearly constant particle size, together with the increasing particle concentration as a function of incubation time, is consistent with the UV–Vis results, where a slight shift in the SPR peak position and an increase in peak intensity are observed, confirming the increase in nanoparticle density. This result differs significantly from our previous study, in which the nanoparticle sizes were more than twice as large, although AgNPs were also synthesized using *Aspergillus niger* [8]. The fungal strains were isolated from different sources and cultured under distinct environmental and temperature conditions, which may have influenced the biosynthesis process and resulted in AgNPs with varying size distributions.

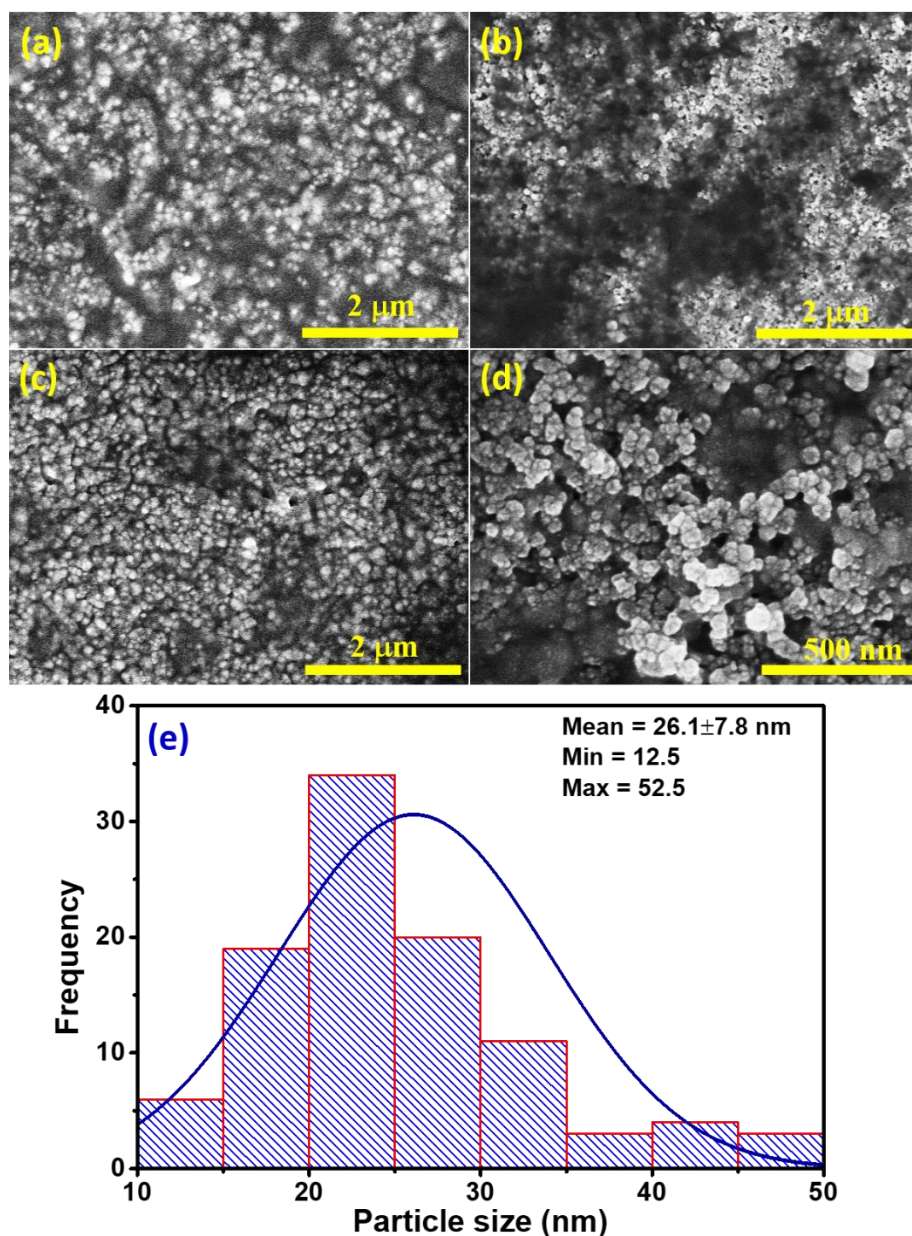


Figure 7. (a–c) SEM images of AgNPs generated from cell-free cultures of *Aspergillus niger* QNUGT6 containing 10 mM AgNO₃ with different incubation times of 24, 48, and 96 h of synthesis. (d) Magnified SEM image. (e) Average particle size distribution of sample (a).

3.6. Antibacterial activity of AgNPs against multidrug-resistant bacteria

The bactericidal efficacy of AgNPs is strongly influenced by particle size, with smaller nanoparticles exhibiting enhanced antimicrobial activity due to larger surface area and stronger interaction with bacterial cell membranes [65–68]. Upon contact, AgNPs can bind to bacterial surfaces, penetrate cells, and release Ag⁺ ions, leading to increased membrane permeability, inhibition of cell division and DNA replication, and ultimately cell death [69,70]. In addition, Ag⁺ ions interact with the negatively charged bacterial cell wall, causing protein denaturation and disrupting proton dynamics [71]. Because silver

has a high affinity for phosphorus-containing biomolecules, Ag^+ can bind to phosphate groups in DNA/RNA structures, causing deformation and hindering replication and transcription, and can also inactivate enzymes, inhibit protein synthesis, hinder DNA replication, and cause microbial cell death [72–74]. This is the core mechanism by which AgNPs effectively kill bacteria.

In this study, the antimicrobial activity of biosynthesized AgNPs against *B. cereus* was evaluated using the disc diffusion method. The results were consistent with those reported in previous studies [64,75]. In Figure 8, AgNPs synthesized after 96 h of incubation exhibited the strongest antibacterial activity, indicating good stability of the nanoparticles produced using this green synthesis method. The *Aspergillus niger* QNUGT6 strain isolated from rice wine yeast therefore shows great potential for the environmentally friendly synthesis of nanomaterials. Furthermore, the *B. cereus* strain used in this study remained highly sensitive to two antibiotics, ampicillin (10 μg) and streptomycin (10 μg).

The MIC and MBC values shown in Table 2 indicate antibacterial effectiveness at a concentration of 2.5 mM. However, these results represent only preliminary evaluations of the nanoparticles in liquid form immediately after synthesis. In future work, we plan to obtain AgNPs in solid form and perform further dilutions to determine MIC and MBC values against a broader range of bacterial species.

Table 2. Minimum inhibitory concentration (MIC) and minimum bactericidal concentration (MBC) of AgNPs after 24 h.

Dilution of AgNPs	MIC (mM)					MBC (mM)	
	10	5	2.5	1.25	0.625	10	5
<i>Bacillus cereus</i>	-	-	+	+	+	-	-

Note: + or - indicate the presence or absence of activity, respectively.

Bacillus cereus is a Gram-positive bacterium characterized by a thick peptidoglycan layer containing phosphate and carboxyl groups, which can increase the negative charge on the bacterial cell surface [76]. This negative surface charge may promote electrostatic interactions with AgNPs, facilitating their attachment to the bacterial cell membrane. The AgNPs synthesized in this study had an average size of 26.1 nm, which may enhance their accumulation on the cell surface and disrupt membrane integrity, thereby affecting cell permeability [67–68].

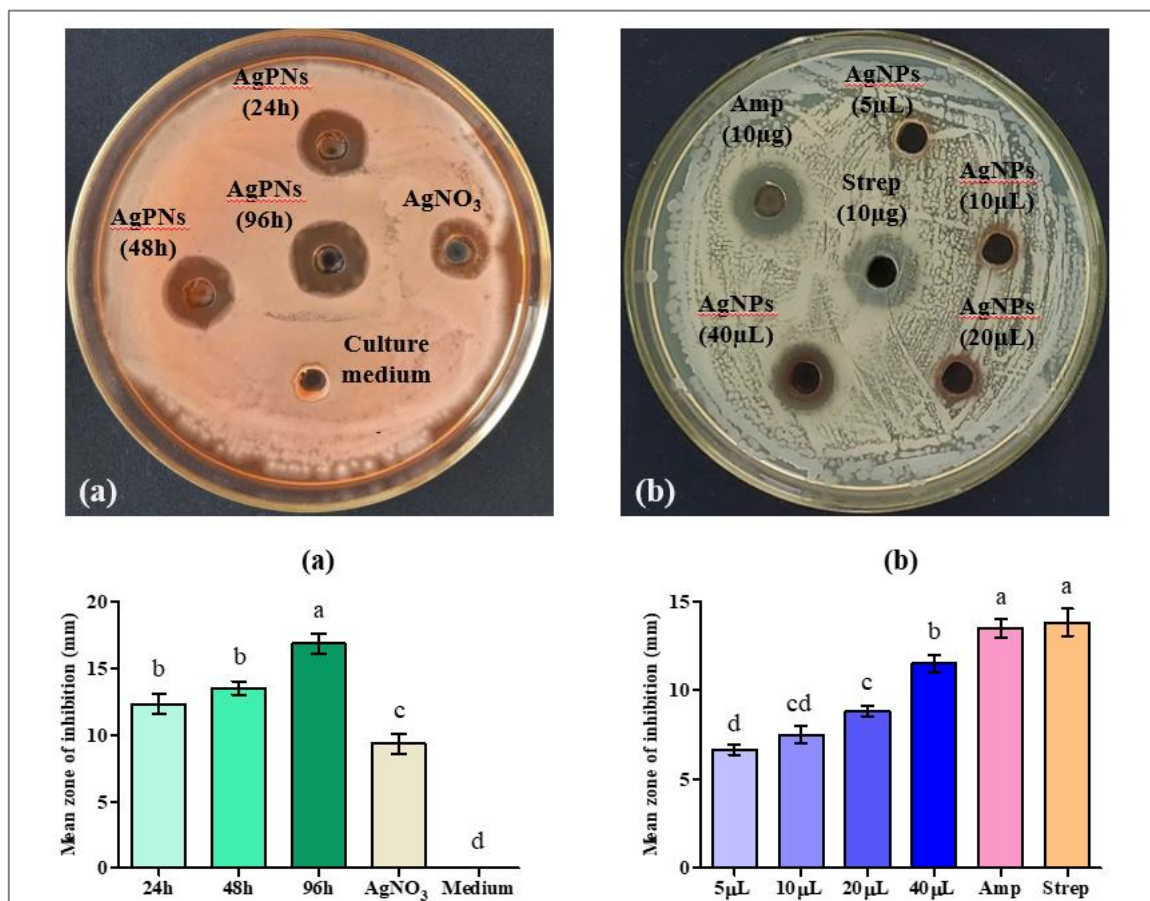
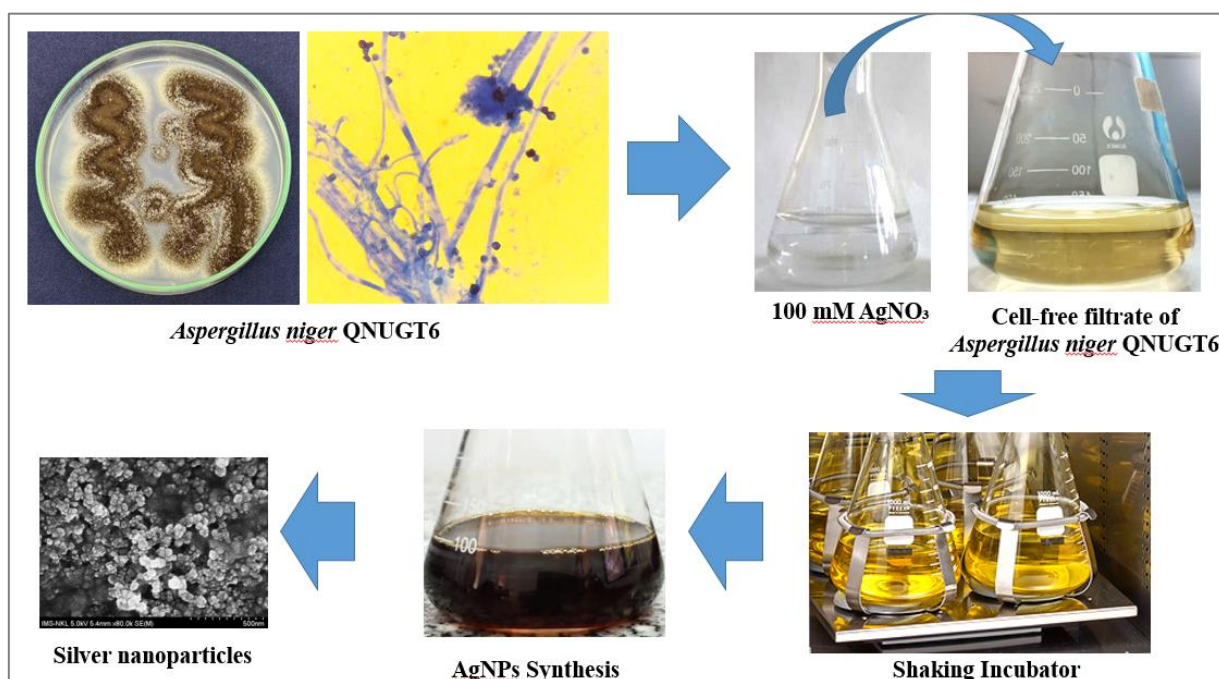


Figure 8. (a) Antibacterial activity of obtained AgNPs after 24, 48, and 96 h of incubation against *B. cereus* by the disk diffusion method on Luria–Bertani agar. (b) Antibacterial activity of obtained AgNPs after 96 h of incubation against *B. cereus* by the disk diffusion method on nutrient agar; ampicillin (Amp 10 μg) and streptomycin (Strep 10 μg) as controls. Results are expressed as mean ± standard deviation (SD); n = 3. Different letters indicate statistically significant differences ($p < 0.05$).

4. Conclusions

In this study, we isolated the *Aspergillus niger* QNUGT6 strain from rice wine yeast. The active metabolites present in the biomass medium of *Aspergillus niger* QNUGT6 were successfully utilized as environmentally friendly reducing agents for the synthesis of AgNPs (Schematic 1). The synthesized AgNPs had an average size of 26.1 ± 7.8 nm, exhibited good stability with various functional groups, and demonstrated antibacterial activity against the foodborne pathogen *Bacillus cereus*. Therefore, these AgNPs could be promising antimicrobial agents for the control of pathogenic bacterial strains.



Schematic 1. AgNPs synthesis process.

Use of generative-AI tools declaration

The authors have not used Artificial Intelligence (AI) tools in the creation of this article.

Conflict of interest

The authors declare no conflict of interest.

Author contributions

Conceptualization: TMDN.; Data curation: NHH. and TMDN.; Formal analysis: NHH. and TMDN.; Methodology: NHH. and TMDN.; Project administration: TMDN.; Writing - original draft: TMDN.; Writing - review and editing: NHH.

References

1. Guilger-Casagrande M, Lima R (2019) Synthesis of silver nanoparticles mediated by fungi: a review. *Front Bioeng Biotech* 7: 287. <https://doi.org/10.3389/fbioe.2019.00287>
2. Muthukrishnan S, Bhakya S, Ramalingam V (2025) Metal nanoparticles synthesis: an overview of different synthesis methods, mode of action and their biomedical application. *Discov Appl Sci* 7: 1079. <https://doi.org/10.1007/s42452-025-07210-y>
3. Gahlawat G, Choudhury AR (2019) A review on the biosynthesis of metal and metal salt nanoparticles by microbes. *RSC Adv* 9: 12944–12967. <https://doi.org/10.1039/C8RA10483B>

4. Jiang H, Wong ACL, Denes FS (2004) Plasma enhanced deposition of silver nanoparticles onto polymer and metal surfaces for the generation of antimicrobial characteristics. *J Appl Polym Sci* 93: 1411–1422. <https://doi.org/10.1002/app.20561>
5. Duran N, Marcato PD, Alves OL, et al. (2005) Mechanistic aspects of biosynthesis of silver nanoparticles by several *Fusarium oxysporum* strains. *J Nanobiotechnol* 3: 8. <https://doi.org/10.1186/1477-3155-3-8>
6. Vijayaram S, Razafindralambo H, Sun YZ, et al. (2024) Applications of green synthesized metal nanoparticles—a review. *Biol Trace Elem Res* 202: 360–386. <https://doi.org/10.1007/s12011-023-03645-9>
7. Dong ZY, Narsing Rao MP, Xiao M, et al. (2017) Antibacterial activity of silver nanoparticles against *Staphylococcus warneri* synthesized using endophytic bacteria by photo-irradiation. *Front Microbiol* 8: 1090. <https://doi.org/10.3389/fmicb.2017.01090>
8. Hieu HN, Trang DTH, Hien VTT, et al. (2022) Microorganism-mediated green synthesis of silver nanoparticles using *Aspergillus niger* and *Bacillus megaterium*. *Dig J Nanomater Bios* 17: 359–367. <https://doi.org/10.15251/DJNB.2022.171.359>
9. Iravani S, Korbekandi H, Mirmohammadi SV, et al. (2014) Synthesis of silver nanoparticles: chemical, physical and biological methods. *Res Pharm Sci* 9: 385–406.
10. Shah M, Fawcett D, Sharma S, et al. (2015) Green synthesis of metallic nanoparticles via biological entities. *Materials (Basel)* 8: 7278–7308. <https://doi.org/10.3390/ma8115377>
11. Kulkarni N, Muddapur U (2015) Biosynthesis of metal nanoparticles: a review. *J Nanotechnol* 2014: 1–8. <https://doi.org/10.1155/2014/510246>
12. Ottoni CA, Simoes MF, Fernandes S, et al. (2017) Screening of filamentous fungi for antimicrobial silver nanoparticles synthesis. *AMB Express* 7: 31. <https://doi.org/10.1186/s13568-017-0332-2>
13. Carrapiço A, Martins MR, Caldeira AT, et al. (2023) Biosynthesis of metal and metal oxide nanoparticles using microbial cultures: mechanisms, antimicrobial activity and applications to cultural heritage. *Microorganisms* 11: 378. <https://doi.org/10.3390/microorganisms11020378>
14. Li J, Li Q, Ma X, et al. (2016). Biosynthesis of gold nanoparticles by the extreme bacterium *Deinococcus radiodurans* and an evaluation of their antibacterial properties. *Int J Nanomed* 11: 5931–5944. <https://doi.org/10.2147/IJN.S119618>
15. Chopra H, Bibi S, Singh I, et al. (2022) Green metallic nanoparticles: biosynthesis to applications. *Front Bioeng Biotechnol* 10: 874742. <https://doi.org/10.3389/fbioe.2022.874742>
16. Singh P, Kim YJ, Zhang D, et al. (2016) Biological synthesis of nanoparticles from plants and microorganisms. *Trends Biotechnol* 34: 588–599. <https://doi.org/10.1016/j.tibtech.2016.02.006>
17. Li N, Siddique A, Liu N, et al. (2025) Global epidemiology and health risks of *Bacillus cereus* infections: special focus on infant foods. *Food Res Int* 201: 115650. <https://doi.org/10.1016/j.foodres.2024.115650>
18. Huang Y, Flint SH, Palmer JS (2020) *Bacillus cereus* spores and toxins—The potential role of biofilms. *Food Microbiol* 90: 103493. <https://doi.org/10.1016/j.fm.2020.103493>
19. Osimani A, Aquilanti L, Clementi F (2018) *Bacillus cereus* foodborne outbreaks in mass catering. *Int J Hosp Manag* 72: 145–153. <https://doi.org/10.1016/j.ijhm.2018.01.013>
20. Parvekar P, Palaskar J, Metgud S, et al. (2020) The minimum inhibitory concentration (MIC) and minimum bactericidal concentration (MBC) of silver nanoparticles against *Staphylococcus aureus*. *Biomaterial Invest Dent* 7: 105–109. <https://doi.org/10.1080/26415275.2020.1796674>

21. Boroumand Moghaddam A, Namvar F, Moniri M, et al. (2015) Nanoparticles biosynthesized by fungi and yeast: a review of their preparation, properties, and medical applications. *Molecules* 20: 16540–16565. <https://doi.org/10.3390/molecules200916540>
22. Sastry M, Ahmad A, Islam Khan M, et al. (2003) Biosynthesis of metal nanoparticles using fungi and actinomycete. *Curr Sci* 85: 162–170. <https://www.jstor.org/stable/24108579>
23. Castro-Longoria E, Moreno-Velázquez SD, Vilchis-Nestor AR, et al. (2012) Production of platinum nanoparticles and nanoaggregates using *Neurospora crassa*. *J Microbiol Biotechnol* 22: 1000–1004. <https://doi.org/10.4014/jmb.1110.10085>
24. Volesky B, Holan ZR (1995) Biosorption of heavy metals. *Biotechnol Progr* 11: 235–250. <https://doi.org/10.1021/bp00033a001>
25. Soni N, Prakash S (2013) Possible mosquito control by silver nanoparticles synthesized by soil fungus (*Aspergillus niger* 2587). *Adv Nanoparticles* 2: 125–132. <https://doi.org/10.4236/anp.2013.22021>
26. Gamorot MD, Amper CD, Marin MB, et al. (2025) Synthesis of silver nanoparticles using *Aspergillus niger* Tiegh and its effects on *Xanthomonas oryzae* pv. *Oryzae*. *Nativa* 13: 38–45. <https://doi.org/10.31413/nat.v13i1.18736>
27. Ninganagouda S, Rathod V, Singh D (2014) Characterization and biosynthesis of silver nanoparticles using a fungus *Aspergillus niger*. *Int Lett Nat Sci* 10: 49–57. <https://doi.org/10.56431/p-hwnei8>
28. Farrag HMM, Mostafa FAAM, Mohamed ME, et al. (2020) Green biosynthesis of silver nanoparticles by *Aspergillus niger* and its antiamebic effect against *Allopathy sp.* trophozoite and cyst. *Exp Parasitol* 219: 108031. <https://doi.org/10.1016/j.exppara.2020.108031>
29. Pasha A, Kumbhakar DV, Sana SS, et al. (2022) Role of biosynthesized Ag-NPs using *Aspergillus niger* (MK503444.1) in antimicrobial, anti-cancer and anti-angiogenic activities. *Front Pharmacol* 12: 812474. <https://doi.org/10.3389/fphar.2021.812474>
30. Khadeeja Yasmeen A, Mohamed S (2019) Biological synthesis of silver nanoparticles using fungus *Aspergillus niger* and its characterization. *Int J Sci Innov Res* 7: 69–74.
31. Gade AK, Bonde P, A. P. Ingle AP, et al. (2008) Exploitation of *Aspergillus niger* for synthesis of silver nanoparticles. *J Biobased Mater Bio* 2: 243–247. <https://doi.org/10.1166/jbmb.2008.401>
32. Singh PP, Chaturvedi S (2020) Biosynthesis of silver nanoparticles through biomass of fungus *Aspergillus niger* and their antibacterial potential. *Int J Mod Trends Sci Technol* 6: 37–42. <https://doi.org/10.46501/IJMTST060609>
33. Vala AK, Chudasama B, Patel RJ (2012) Green synthesis of silver nanoparticles using marine-derived fungus *Aspergillus niger*. *Micro Nano Letters* 7: 859–862. <https://doi.org/10.1049/mnl.2012.0403>
34. Patel D, Jha R (2021) Biosynthesis, characterization, and antimicrobial activity of silver nanoparticles by *Aspergillus niger* isolated from the rotten onion. *Int J Curr Microbiol Appl Sci* 10: 489–500. <https://doi.org/10.20546/ijcmas.2021.1010.059>
35. Tejomoortula SR, Bhargavi A, Radhakrishna A, et al. (2023) *Aspergillus niger* mediated green synthesis of silver nanoparticles and activity against *Aspergillus fumigatus*. *Eur J Biotechnol Biosci* 11: 74–77.

36. Hussein TA, Abbass IJ, Razaq AA, et al. (2024) Biosynthesis of silver nanoparticles using *Aspergillus niger* isolated from soil and studying its antimicrobial effect against some multidrug-resistant bacterial species and candida albican. *Vet Med Public Health J* 5: 142–152. <https://doi.org/10.31559/VMPH2024.5.2.15>
37. Elegbede JA, Lateef A, Azeez MA, et al. (2028) Fungal xylanases-mediated synthesis of silver nanoparticles for catalytic and biomedical applications. *IET Nanobiotechnol* 12: 857–863. <https://doi.org/10.1049/iet-nbt.2017.0299>
38. Li G, He D, Qian Y, et al. (2012) Fungus-mediated green synthesis of silver nanoparticles using *Aspergillus terreus*. *Int J Mol Sci* 13: 466–476. <https://doi.org/10.3390/ijms13010466>
39. Malik MA, Wani AH, Bhat MY, et al. (2024) Fungal-mediated synthesis of silver nanoparticles: a novel strategy for plant disease management. *Front Microbiol* 15: 1399331. <https://doi.org/10.3389/fmicb.2024.1399331>
40. Lotfy WA, Alkersh BM, Sabry SA, et al. (2021) Biosynthesis of silver nanoparticles by *Aspergillus terreus*: characterization, optimization, and biological activities. *Front Bioeng Biotechnol* 9: 633468. <https://doi.org/10.3389/fbioe.2021.633468>
41. Nout MJR, Aidoo KE (2002) Asian fungal fermented food, *The Mycota X, Industrial Applications*, Berlin, Heidelberg: Springer, 23–47. Springer. https://doi.org/10.1007/978-3-642-11458-8_2
42. Chen B, Wu Q, Xu Y (2014) Filamentous fungal diversity and community structure associated with the solid state fermentation of Chinese Maotai-flavor liquor. *Int J Food Microbiol* 179: 80–84. <https://doi.org/10.1016/j.ijfoodmicro.2014.03.011>
43. Xu-Cong Lv, Huang ZQ, Zhang W, et al. (2012) Identification and characterization of filamentous fungi isolated from fermentation starters for Hong Qu glutinous rice wine brewing. *J Gen Appl Microbiol* 58: 33–42. <https://doi.org/10.2323/jgam.58.33>
44. Rai M, Ingle AP, Gade A, et al. (2015) Synthesis of silver nanoparticles by *Phoma gardeniae* and in vitro evaluation of their efficacy against human disease-causing bacteria and fungi. *IET Nanobiotechnol* 9: 71–75. <https://doi.org/10.1049/iet-nbt.2014.0013>
45. Siddiqi KS, Husen A, Rao RAK (2018) A review on biosynthesis of silver nanoparticles and their biocidal properties. *J Nanobiotechnol* 16: 14. <https://doi.org/10.1186/s12951-018-0334-5>
46. Wypij M, Czarnecka J, Swiecimska M, et al. (2018) Synthesis, characterization and evaluation of antimicrobial and cytotoxic activities of biogenic silver nanoparticles synthesized from *Streptomyces xinghaiensis* OF1 strain. *World J Microbiol Biotechnol* 34: 23. <https://doi.org/10.1007/s11274-017-2406-3>
47. Chowdhury S, Basu A, Kundu S (2014) Green synthesis of protein capped silver nanoparticles from phytopathogenic fungus *Macrophomina phaseolina* (Tassi) Goid with antimicrobial properties against multidrug-resistant bacteria. *Nanoscale Res Lett* 9: 365. <https://doi.org/10.1186/1556-276X-9-365>
48. Wang D, Xue B, Wang L, et al. (2021) Fungus-mediated green synthesis of nano-silver using *Aspergillus sydowii* and its antifungal/antiproliferative activities. *Sci Rep* 11: 10356. <https://doi.org/10.1038/s41598-021-89854-5>
49. Gupta RK, Kumar V, Gundampati RK, et al. (2017) Biosynthesis of silver nanoparticles from the novel strain of *Streptomyces* Sp. BHUMBU-80 with highly efficient electroanalytical detection of hydrogen peroxide and antibacterial activity. *J Environ Chem Eng* 5: 5624–635. <https://doi.org/10.1016/j.jece.2017.09.029>

50. Saxena J, Sharma P, Singh A (2017) Biomimetic synthesis of AgNPs from *Penicillium chrysogenum* strain FGCC/BLS1 by optimising physico-cultural conditions and assessment of their antimicrobial potential. *IET Nanobiotechnol* 11: 576–583. <https://doi.org/10.1049/iet-nbt.2016.0097>
51. Naseer QA, Xue X, Wang X, et al. (2021) Synthesis of silver nanoparticles using *Lactobacillus bulgaricus* and assessment of their antibacterial potential. *Braz J Biol* 82: e232434. <https://doi.org/10.1590/1519-6984.232434>
52. Fouda A, Awad MA, AL-Faifi ZE, et al. (2022) *Aspergillus flavus*-mediated green synthesis of silver nanoparticles and evaluation of their antibacterial, anti-*Candida*, acaricides, and photocatalytic activities. *Catalysts* 12: 462. <https://doi.org/10.3390/catal12050462>
53. Harutyunyan A, Hambardzumyan A, Gabrielyan L, et al. (2025) Silver nanoparticles fabricated using phycocyanin from *Arthrospira platensis*: green synthesis, physicochemical characterization, and biological activities. *Microb Cell Fact* 24: 249. <https://doi.org/10.1186/s12934-025-02871-1>
54. Saif FA, Yaseen SA, Alameen AS, et al. (2021) Identification and characterization of *Aspergillus* species of fruit rot fungi using microscopy, FT-IR, Raman and UV-Vis spectroscopy. *Spectrochim Acta A Mol Biomol Spectrosc* 246: 119010. <https://doi.org/10.1016/j.saa.2020.119010>
55. Rohman A, Windarsih A, Lukitaningsih E, et al. (2019) The use of FTIR and Raman spectroscopy in combination with chemometrics for analysis of biomolecules in biomedical fluids: a review. *Biomed Spectrosc Im* 8: 55–71. <https://doi.org/10.3233/BSI-200189>
56. Bozanic DK, Trandafilović LV, Luyt AS, et al. (2010) Green synthesis and optical properties of silver-chitosan complexes and nanocomposites. *React Funct Polym* 70: 869–873. <https://doi.org/10.1016/j.reactfunctpolym.2010.08.001>
57. Jaidev LR, Narasimha G (2010) Fungal mediated biosynthesis of silver nanoparticles, characterization and antimicrobial activity. *Colloid Surface B* 81: 430–433. <https://doi.org/10.1016/j.colsurfb.2010.07.033>
58. Trofimov BA, Sinegovskaya LM, Gusarova NK (2009) Vibrations of the S–S bond in elemental sulfur and organic polysulfides: a structural guide. *J Sulfur Chem* 30: 518–554. <https://doi.org/10.1080/17415990902998579>
59. Chena X, Yuan X, Yu Z, et al. (2025) Ginkgo biloba-derived biogenic silver nanoparticles suppress the proliferation of C6 glioma cells via apoptosis, cell cycle arrest, and anti-migratory activity. *Arab J Chem* 19: 7612025. https://doi.org/10.25259/AJC_761_2025
60. Aguirre DPR, Loyola EF, Salcido NMDF, et al. (2020) Comparative antibacterial potential of silver nanoparticles prepared via chemical and biological synthesis. *Arab J Chem* 13: 8662–8670. <https://doi.org/10.1016/j.arabjc.2020.09.057>
61. Khaled SYAB, Annadurai S, et al. (2024) Green synthesis and characterization of silver nanoparticles using *Moringa Peregrina* and their toxicity on MCF-7 and Caco-2 human cancer cells. *Int J Nanomed* 19: 3891–3905. <https://doi.org/10.2147/IJN.S451694>
62. Nitin KS, Jyotsna V, et al. (2022) Green route synthesis and characterization techniques of silver nanoparticles and their biological adeptness. *ACS Omega* 7: 27004–27020. <https://doi.org/10.1021/acsomega.2c01400>
63. Shivanjali EA, Jyotsna K (2024) Green and chemical syntheses of silver nanoparticles: Comparative and comprehensive study on characterization, therapeutic potential, and cytotoxicity. *Eur J Med Chem Rep* 11: 100168. <https://doi.org/10.1016/j.ejmcr.2024.100168>

64. Amargeetha A, Velavan S (2018) X-ray diffraction (XRD) and energy dispersive spectroscopy (EDS) analysis of silver nanoparticles synthesized from *Erythrina indica* flowers. *NanoSci Technol* 5: 1–5. <https://doi.org/10.15226/2374-8141/5/1/00152>
65. Thiel J, Pakstis L, Buzby S, et al. (2007) Antibacterial properties of silver-doped titania. *Small* 3: 799–803. <https://doi.org/10.1002/sml.200600481>
66. Martinez-Castanon GA, Niño-Martínez N, Martínez-Gutierrez F, et al. (2008) Synthesis and antibacterial activity of silver nanoparticles with different sizes. *J Nanopart Res* 10: 1343–1348. <https://doi.org/10.1007/s11051-008-9428-6>
67. Inphonlek S, Pimpha N, Sunintaboon P (2010) Synthesis of poly (methyl methacrylate) core/chitosan-mixed-polyethyleneimine shell nanoparticles and their antibacterial property. *Colloid Surface B* 77: 219–226. <https://doi.org/10.1016/j.colsurfb.2010.01.029>
68. Xiu ZM, Zhang QB, Puppala HL, et al. (2012) Negligible particle-specific antibacterial activity of silver nanoparticles. *Nano Lett* 12: 4271–4275. <https://doi.org/10.1021/nl301934w>
69. Khanra K, Panja S, Choudhuri I, et al. (2015) Evaluation of antibacterial activity and cytotoxicity of green synthesized silver nanoparticles using *Scoparia dulcis*. *Nano Biomed Eng* 7: 128–133. <https://doi.org/10.5101/nbe.v7i3.p128-133>
70. Wang D, Xue B, Wang L, et al. (2021) Fungus-mediated green synthesis of nano-silver using *Aspergillus sydowii* and its antifungal/antiproliferative activities. *Sci Rep* 11: 10356. <https://doi.org/10.1038/s41598-021-89854-5>
71. Singh A, Jain D, Upadhyay MK, et al. (2010) Green synthesis of silver nanoparticles using *Argemone Mexicana* leaf extract and evaluation of their antimicrobial activities. *Dig J Nanomater Biostructures* 5: 483–489.
72. Baker S, Harini BP, Rakshith D, et al. (2013) Marine microbes: invisible nanofactories. *J Pharm Res* 6: 383–388. <https://doi.org/10.1016/j.jopr.2013.03.001>
73. Vicas SI, Cavalu S, Laslo V, et al. (2019) Growth, photosynthetic pigments, phenolic, glucosinolates content and antioxidant capacity of broccoli sprouts in response to nanoselenium particles supply. *Not Bot Horti Agrobo* 47: 821–828. <https://doi.org/10.15835/nbha47311490>
74. Mikhailova EO (2025) Green silver nanoparticles: an antibacterial mechanism. *Antibiotics* 14: 5. <https://doi.org/10.3390/antibiotics14010005>
75. Hoang NH, Nguyen VN, Nguyen TT, et al. (2023) Impact of microwave synthesis time on the shape of silver nanostructures and their antibacterial activity. *J Met Mater Miner* 33: 101–106. <https://doi.org/10.55713/jmmm.v33i1.1631>
76. Baron S (1996) *Medical Microbiology*, 4 Eds., Galveston: University of Texas Medical Branch.



AIMS Press

© 2026 the Author(s), licensee AIMS Press. This is an open access article distributed under the terms of the Creative Commons Attribution License (<http://creativecommons.org/licenses/by/4.0>)